Homoleptic Cuprates(II) with Multiply Deprotonated α-Cyclodextrin Ligands[**]

Peter Klüfers,[*] Holger Piotrowski and Jürgen Uhlendorf

Abstract: In the presence of cupric ions, α-cyclodextrin (α-CD) is multiply deprotonated in alkaline aqueous solution. With lithium or sodium as the counterions, trinuclear sandwich-type cuprate ions of the formula $[Cu_3(\alpha\text{-CDH}_{-6})_2]^{6-}$ are formed (**1** and **2**), whereas dinuclear $[Cu_2(\alpha\text{-CDH}_{-4})_2]^{4-}$ ions are isolated in the form of the potassium (**3a**) and the rubidium salts (**3b**). The structures of the cyclodextrinatocuprate ions resemble cylinders, since the usual conical shape of a cyclodextrin is altered due to the formation of shorter hydrogen bonds on the O2/O3 rim of the α-cyclodextrin torus. Despite anion formation, the cavity of the cyclodextrin is still hydrophobic, giving rise to the intercalation of acetone guests in **2** and **3**.

Keywords
copper · cuprates · cyclodextrins · structure elucidation

Introduction

Stable bis(diolato(2−))cuprates(II) may be synthesized in aqueous alkaline solution from a cupric salt and a simple diol as well as a suitable, that is, non-reducing, carbohydrate (derivative). Bis(diolato)cuprates are thermodynamically stable;[1] moreover, they are accessible from both 1,2-[2] and 1,3-diols.[3] Polyols with three or more hydroxy groups arranged in a suitable configuration ("higher polyols") exhibit an even more complicated coordination chemistry.[4] Obviously, the most important individual factor that may interfere with the deprotonation of the diol functions and hence the complexation of metal ions with higher polyols is the potential formation of intramolecular hydrogen bonds in the deprotonated polyolato ligand.[5]

An understanding of the rules governing the particular deprotonation and complexation pattern exhibited by a polyfunctional polyol is of technical interest: the polysaccharide cellulose acts as a polymeric ligand in the so-called "Normann's compound" (sodium cupric cellulose), which is a key intermediate in the alkaline variant of the cuprammonium process used for the fabrication of cellulosic dialysis membranes used in uremia therapy.[6] Starting with a solution of cellulose in Schweizer's reagent (cupric hydroxide in aqueous ammonia), in which single-stranded cellulose is bound to ammine copper units, Normann's compound is precipitated by wet spinning with aqueous sodium hydroxide as the precipitating liquid. Elemental analysis of the blue films gives the approximate formula $Na_2[Cu(Glc_CH_{-2})_2]$ ($Glc_C \equiv \beta$-1,4-linked D-anhydroglucose unit of cellulose) for the anhydrous material.[7] However, the structure of this polysaccharide–metal complex is still unknown. The investigation of oligosaccharide–metal complexes may be a promising approach to perceive structural principles, but even these low-molecular compounds have not yet been crystallized.[8] However, this does not apply with a cyclodextrin as the oligosaccharide component. The substantially greater tendency of cyclodextrins towards crystallization is retained when they act as ligands in a cupric complex. The very first cyclodextrin–metal complex described was in fact a cuprate.[9] With this work, we submit a more comprehensive study of cyclodextrinatocuprates, which contributes to the knowledge of the competing factors in oligosaccharide metalate formation. The compounds in question are composed of pairs of deprotonated α-cyclodextrin (α-CD) rings, which enclose cupric ions in a sandwich-type manner. However, in $Li_3[Li_3Cu_3(\alpha\text{-CDH}_{-6})_2]\cdot 41\,H_2O$ (**1**), $Na_3[Na_3Cu_3(\alpha\text{-CDH}_{-6})_2]\cdot$acetone$\cdot 32\,H_2O$ (**2**) and $A_4[Cu_2(\alpha\text{-CDH}_{-4})]\cdot x\,H_2O\cdot 2$ acetone (**3a**, A = K, $x = 23$) (**3b**, A = Rb, $x = 21$), the number of cupric ions complexed is less than the number of bisdiol moieties available, which indicates that the rules of complex formation are more complicated than those for a simple monosaccharide ligand.

Experimental Procedure

Dark blue crystals of the title compounds were prepared by the reaction of α-cyclodextrin (1.946 g, 2 mmol), cupric nitrate trihydrate (0.725 g, 3 mmol) and the required quantity of a stock solution of the respective alkali hydroxide (12 mmol LiOH or NaOH, or 8 mmol KOH or RbOH) in 20 mL water. On diffusion of acetone vapour crystallization takes place within a few days.

Suitable crystals were investigated with the Stoe Imaging Plate Diffraction System ($Mo_{K\alpha}$, $\lambda = 71.069$ pm). The structures were solved, refined, analyzed and depicted with the programs SHELXS, SHELXL, PLATON and SCHAKAL. R values are defined by $R(F) = \sum\Delta_1/\sum|F_o|$ with $\Delta_1 = ||F_o| - |F_c||$, $wR(F^2) = \{\sum(w\Delta_2^2)/\sum w(F_o^2)^2\}^{1/2}$ with $\Delta_2 = |F_o^2 - F_c^2|$, weights being defined by $w^{-1} = \sigma^2(F_o^2) + (xP)^2 + yP$; $3P = \max(F_o^2,0) + 2F_c^2$. The

---

[*] Prof. Dr. P. Klüfers, Dipl.-Chem. H. Piotrowski, Dr. J. Uhlendorf
Institut für Anorganische Chemie der Universität
Engesserstr., Gebäude 30.45, D-76128 Karlsruhe (Germany)
Fax: Int. Code +(721)608-2135
e-mail: kluefers@achibm2.chemie.uni-karlsruhe.de

[**] Polyol Metal Complexes, Part 22. Part 21: J. Burger, P. Klüfers, *Angew. Chem. Int. Ed. Engl.* **1997**, *36*, Issue 7.

Table 1. Crystal structure data of **1**–**3** [a].

	1	**2**	**3a**	**3b**
formula	$C_{72}H_{108}Cu_3Li_6O_{60}$	$C_{72}H_{108}Cu_3Na_6O_{60}$	$C_{72}H_{112}Cu_2K_4O_{60}$	$C_{72}H_{112}Cu_2Rb_4O_{60}$
water content; guest molecules	40.9(6) = 25.4%	31.9(4) = 19.9%; 1 C_3H_6O	23.0(3) = 15.1%; 2 C_3H_6O	21.4(2) = 13.3%; 2 C_3H_6O
M_r (g mol^{-1})	2902.722	2894.958	2751.642	2908.296
crystal system; class	monoclinic; 2-C_2	monoclinic; 2-C_2	orthorhombic; 222-D_2	orthorhombic; 222-D_2
space group	$P2_1$	$P2_1$	$P2_12_12_1$	$P2_12_12_1$
a (pm)	1718.2(3)	1633.1(2)	1611.9(2)	1608.1(2)
b (pm)	5188.7(5)	3386.2(4)	2712.8(5)	2717.2(3)
c (pm)	1720.7(2)	2500.9(3)	2804.8(16)	2801.2(3)
β (°)	116.285(11)	105.520(10)	90	90
V (10^6 pm^3); Z	13755(3); 4	13326(3); 4	12265(8); 4	12240(2); 4
ρ_{calc} (g cm^{-3}; μ (mm^{-1})	1.4017(3); 0.579	1.4430(3); 0.605	1.4902(10); 0.595	1.5782(3); 2.041
crystal size (mm)	0.10 × 0.10 × 0.07	0.20 × 0.20 × 0.20	0.20 × 0.20 × 0.10	0.23 × 0.12 × 0.08
T (K)	293(3)	190(3)	190(3)	220(3)
crystal-to-plate distance (mm)	100	100	90	80
ϕ range (°); increment	0–99.2; 0.4	0–106.4; 0.4	0–140; 1.0	0–105.6; 0.4
exposure (min)	6	8	4	8
no. refls for unit cell let	1113	464	1269	553
2θ range (°)	3–42	6–42	6–42	3–42
refls collected	35472	29602	38491	29120
unique refls	21331	17145	13103	12001
R_{int}	0.0814	0.0641	0.0332	0.0590
mean $\sigma(I)/I$	0.0675	0.0851	0.0252	0.0556
observed refls $I \geq 2\sigma(I)$	20024	13095	12295	10381
parameters; restraints	1485; 1	1469; 1	729	730; 1
$wR(F^2)$	0.2271	0.2567	0.2016	0.2101
$R(F)_{obs}$	0.1022	0.0907	0.0718	0.0770
S	1.077	1.063	1.037	1.014
max shift/error	0.001	0.001	0.001	0.001
$\|\Delta\rho\|_{max}$ (10^{-6} e pm^{-3})	1.334	1.122	2.000	1.231
x, y weighting	0.1658, 114.1341	0.1369; 97.1907	0.1258; 53.1570	0.1334, 55.5472
absolute structure [b]	0.07(2)	−0.01(2)	0.01(2)	0.038(12)

[a] C-bonded H atoms fixed (C–H = 96 pm), one common U_{iso}. [b] H. D. Flack, *Acta Crystallogr. Sect. A* **1983**, *39*, 876–881.

"goodness of fit" is defined by $S = \{\sum(w\Delta_2/(N_{hkl} - N_{parameters})\}^{1/2}$. Crystallographic parameters are given in Table 1.[10]

Throughout the text, standard deviations of the last digit from X-ray refinement are given in brackets; mean values are given as a numerical value ± standard deviation of the mean. The water content given in Table 1 is the sum of the population parameters of the oxygen atoms that have been assigned as water molecules; the standard deviation of the water content given is the sum of the standard deviations of the population parameters less than 1 of these water positions. With the exception of the packing diagrams (Figures 5 and 6), all figures are drawn on the same scale. Atoms of the cyclodextrin rings are numbered in the form C307 or O512. Here, the first numeral refers to the usual numbering of hexose atoms (Scheme 1), while the following two digits represent the number of the anhydroglucose unit as specified in Schemes 2–4.

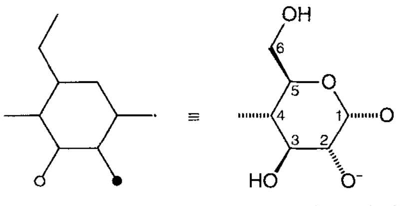

Scheme 1. Encoding of the structure of an anhydroglucose unit of α-cyclodextrin and its locus of deprotonation as used in Schemes 2–4.

To avoid confusion, throughout the text the term "donor" is used in equivalence to "hydrogen-bond donor group", though an electron-pair donor atom in a coordinative bond is termed "ligator" for short.

Results

Cuprate(II) solutions with α-cyclodextrin: Aqueous solutions of α-cyclodextrin containing a threefold molar quantity of cupric nitrate reacted with excess alkali hydroxide to yield both a deep blue cuprate(II) solution and a precipitate of cupric hydroxide. The amount of dissolved copper was determined from the mass of the precipitate. With the hydroxides of lithium, sodium and potassium, a constant amount of 1.5 mol dissolved Cu^{II} per mole of α-cyclodextrin resulted, that is, trinuclear double tori of the formula $[Cu_3(\alpha\text{-CDH}_{-6})_2]^{6-}$, which constitute the crystal structures of **1** and **2**, appear to be the main constituents of all of the aqueous alkaline copper-saturated α-cyclodextrin solutions investigated. On diffusion of acetone vapour into the mixtures, blue crystals of **1** and **2** formed from the respective solutions, whereas this method failed for the preparation of crystals from solutions containing potassium.

Solutions with a 1:1 ratio of copper and α-cyclodextrin, that is, with a higher amount of saccharide, behave differently with the three alkali hydroxides investigated. Lithium and sodium hydroxide effected the formation of crystals of **1** and **2**, respectively, leaving one-third of the cyclodextrin tori uncomplexed. On the other hand, in the presence of potassium hydroxide, blue crystals of **3a**, a cuprate(II) of lower copper content, form from the solutions.

The cyclodextrinatocuprate cylinders: The structural description is focussed on the interplay of three main factors contributing to the actual structure of the cuprate entities: 1) the formation of thermodynamically stable bis(diolato)cuprate(II) ions, 2) counterion binding to the double tori at multidentate binding sites preferentially located at OH groups, 3) formation of intramolecular O–H···O⁻ bonds. Steric requirements of the obviously flexible α-cyclodextrin tori[11] have not been recognized as competing markedly with these energetically more significant contributions.

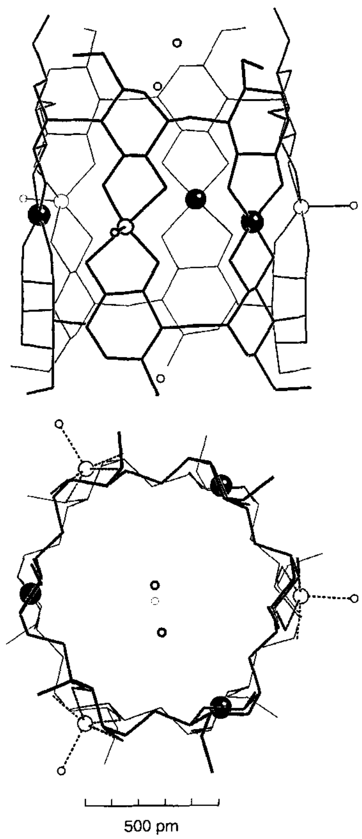

Figure 1. SCHAKAL drawing of the structure of one of two symmetrically independent $[Li(H_2O)_3Cu_3(\alpha\text{-}CDH_{-6})_2]^{3-}$ ions of **1**; filled circles: Cu, empty circles: Li and H_2O. Top: view almost perpendicular to the cylinder axis; bottom: view onto the Cu_3 plane. All the water molecules close to the cavity of the cylinders have been drawn; note the coordination polyhedra of the lithium atoms being midway between square planar and trigonal bipyramidal; Cu–O bonds have been omitted from the bottom view. Distances (pm) (cf. Scheme 2 for atom numbering): from Cu1 to: O307 192.6(10), O301 193.3(10), O207 195.0(9), O201 195.9(9); from Cu2 to: O303 192.5(11), O209 194.0(10), O203 194.8(10), O309 195.9(10); from Cu3 to: O211 193.6(12), O311 194.3(10), O305 194.9(10), O205 196.0(11); from Cu4 to: O313 192.6(10), O319 193.0(10), O213 194.0(8), O219 194.6(8); from Cu5 to: O315 192.9(10), O321 194.2(9), O215 195.3(11), O221 196.3(11); from Cu6 to: O317 189.0(12), O323 190.2(10), O223 195.2(10), O217 196.1(10).

Table 2. Hydrogen bonded O–O distances (pm) (the assignment of letters *a*–*d* refers to Schemes 2–4); mean values (pm): ***a***: 262 ± 5 (**1**), 272 ± 13 (**2**), 255 ± 4 (**3a**); ***b***: 269 ± 6 (**1**), 265 ± 8 (**2**), 276 ± 5 (**3a**); mean of ***a*** and ***b*** ($O-H\cdots O^-$ bonds): 266 ± 6 (**1**), 268 ± 11 (**2**), 266 ± 11 (**3a**); ***c***: 301 ± 9 (**3a**), 300 ± 11 (**3b**); ***d***: 293 ± 8 (**3a**), 291 ± 7 (**3b**); overall mean values for **3** are listed in Table 3.

		1	**2**			**3a**	**3b**
O202···O303	***a***	271(3)	255(2)	O203···O304	***a***	256.1(7)	256.1(12)
O204···O305	***a***	260(2)	269(2)	O206···O301	***a***	259.1(8)	255.3(12)
O206···O301	***a***	267(3)	294(2)	O208···O307	***a***	249.3(8)	250.2(12)
O208···O307	***a***	266(2)	263(2)	O211···O310	***a***	256.7(7)	257.6(10)
O210···O309	***a***	260(3)	269(3)	O302···O201	***b***	281.4(7)	291.4(12)
O212···O311	***a***	254(3)		O305···O204	***b***	280.8(7)	281.7(12)
O214···O315	***a***	267(2)	265(2)	O309···O210	***b***	272.2(7)	273.2(11)
O216···O317	***a***	263(3)	267(2)	O312···O207	***b***	271.3(8)	268.1(12)
O218···O313	***a***	256(2)	299(3)	O303···O309	***c***	310.7(8)	313.2(12)
O220···O319	***a***	260(3)	268(2)	O306···O312	***c***	308.6(7)	308.7(10)
O222···O321	***a***	256(3)	267(2)	O308···O302	***c***	290.5(8)	292.7(11)
O224···O323	***a***	269(3)		O311···O305	***c***	292.7(7)	286.5(10)
O302···O201	***b***	267(2)	271(2)	O202···O303	***d***	296.1(8)	292.0(12)
O304···O203	***b***	264(3)	259(3)	O205···O306	***d***	279.8(8)	280.3(12)
O306···O205	***b***	276(3)	255(2)	O209···O308	***d***	300.6(8)	293.0(12)
O308···O209	***b***	272(3)	257(2)	O212···O311	***d***	294.6(8)	299.2(12)
O310···O211	***b***	274(3)	275(2)				
O312···O207	***b***	271(3)	256(2)				
O314···O213	***b***	272(3)	271(2)				
O316···O215	***b***	276(3)	271(2)				
O318···O217	***b***	264(3)	257(2)				
O320···O221	***b***	272(3)	277(2)				
O322···O223	***b***	269(3)	270(2)				
O324···O219	***b***	256(3)	255(2)				

Tricuprate(II) ions of **1** exhibit almost perfect noncrystallographic C_3 symmetry (Figure 1). Both tight binding of lithium ions and formation of the maximum number of strong, isolated $O-H\cdots O^-$ bonds (Table 2, Scheme 2) demonstrates the synergetic interconnection of the factors mentioned above in the case of **1**. Besides three bis(diolato)cuprate(II) moieties, three tetradentate O_4 ligator sets are present to bind three lithium atoms, each of which exhibits fivefold coordination owing to bonding of water as a fifth ligand. The three lithium-bound aqua ligands are directed towards the outside of the polyolatocuprate cylinders (cf. the β-cyclodextrin homologue[9a] with in-torus bound aqua ligands). Because of the lack of further ligands at the cupric centres, the cavities of the cylinders are free from tightly bound solvent molecules. In addition to the well-defined anionic $[Li_3(H_2O)_3Cu_3(\alpha\text{-}CDH_{-6})_2]^{3-}$ subunits, the position of only one further, tetrahedrally aqua-ligated, lithium ion serving as a counterion has been resolved from the structural analysis.

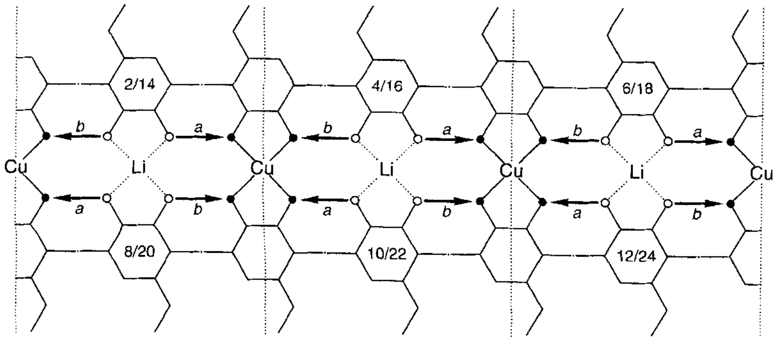

Scheme 2. Cyclodextrin numbering scheme and intramolecular hydrogen bonds in the structure of the cuprate(II) ions in **1**, depicted as arrows from donor to acceptor groups; donor-acceptor distances for ***a*** (O2 donors) and ***b*** (O3 donors) are given in Table 2.

The topography of the cylindrical anions of the homologous sodium compound **2** is closely related to that of **1**. In Scheme 3, two of the three segments resemble the view of **1** given in Scheme 2. C_3 symmetry is broken in the third segment, in which a sodium ion has not assembled diol groups to construct a macrocyclic-ligand-type O_4 ligator set. Instead, a further counterion binding site is provided at a copper-coordinating alkoxo oxygen atom at the expense of an $O-H\cdots O^-$ bond, that is, a type of binding site common with simple polyolato metallate structures—but unique in this investigation—is present. Furthermore, the alkoxo-bound sodium ion is attached inside the tricuprate cylinder, giving rise to intercalation of not only an aqua ligand, accompanied by a further hydrogen-bonded water molecule, but also of an acetone molecule. The acetone does not act as a typical van-der-Waals-bonded guest in a cyclodextrin cavity, but is fixed by a well-defined Na–O contact (Figure 2).

The structure of the isotypic dinuclear cuprates **3a** and **3b** differs markedly from the cation-tricuprate assemblies of **1** and **2** (Figure 3). In the less deprotonated cyclodextrin ligands, besides isolated $O-H\cdots O^-$ bonds, short cooperative hydrogen-bond sequences can be derived from the respective $O\cdots O$ distances (Table 2, Scheme 4). To accomplish the specific hydrogen-bond pattern observed, a slight counterclockwise rotation of the uncomplexed anhydroglucose rings is required (cf. Figure 3, top) bringing O3 hydroxy groups of facing diol moieties into closer contact.[12] Thus, hydrogen bonds of type *c* (Table 2, Scheme 4) are

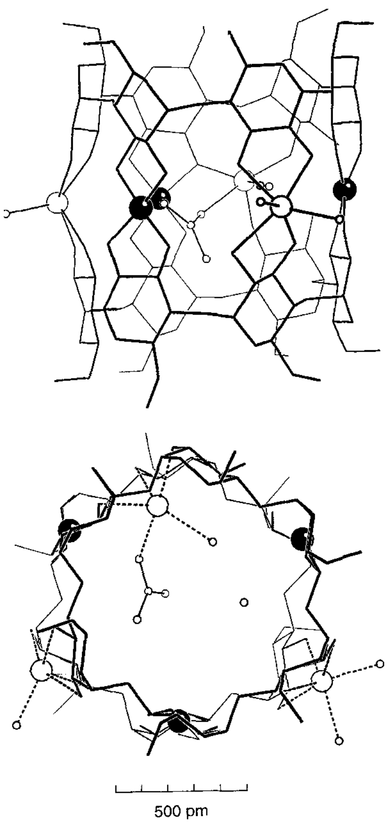

Figure 2. Compound **2**. SCHAKAL drawing of the structure of one of two symmetrically independent $[Cu_3(\alpha\text{-CDH}_{-6})_2]^{6-}$ ions including three multidentate sodium ions and further ligands of the latter; filled circles: Cu; empty circles: Na, H_2O and acetone. Top: view almost perpendicular to the cylinder axis; bottom: view onto the Cu_3 plane. All water and acetone molecules inside the cavity have been drawn. Note the connection of the intercalated molecules to the inside-directed sodium ion, the remainder of the cavity being utterly free of further guest molecules. Distances (pm) (cf. Scheme 3 for atom numbering): from Cu1 to: O201 194.0(13), O207 194.5(13), O301 194.8(14), O307 198.2(14); from Cu2 to: O309 189(2), O203 192.7(15), O209 194.3(15), O303 196(2); from Cu3 to: O311 193.6(11), O211 196.5(11), O205 197.3(13), O305 197.4(11); from Cu4 to: O219 192.5(14), O313 193.8(15), O213 194.8(13), O319 195.9(14); from Cu5 to: O315 192.9(13), O321 194.8(13), O215 195.4(12), O221 195.7(15); from Cu6 to: O323 192.3(11), O317 194.3(11), O217 195.3(12), O223 196.1(11). Pyranose ring number and cone angle (°) according to Table 3, footnote [a]: 1 89.2, 2 85.4, 3 79.0, 4 88.9, 5 87.9, 6 85.4, 7 87.0, 8 87.3, 9 78.2, 10 81.0, 11 83.2, 12 72.7, 13 87.1, 14 81.0, 15 83.6, 16 87.9, 17 89.4, 18 86.5, 19 88.4, 20 89.3, 21 86.2, 22 81.1, 23 85.8, 24 74.7.

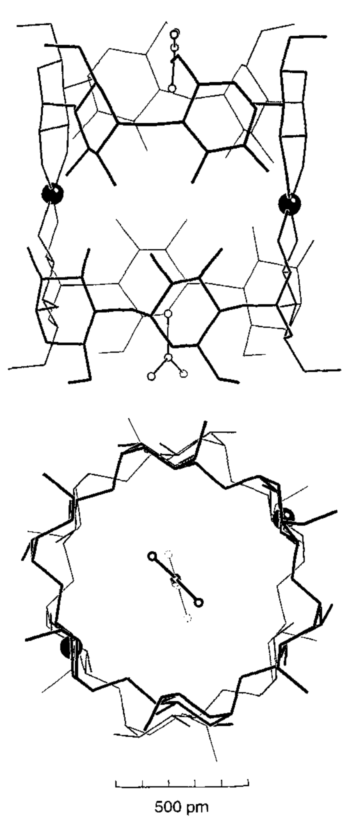

Figure 3. SCHAKAL drawing of the structure of the $[Cu_2(\alpha\text{-CDH}_{-4})_2]^{4-}$ ion of **3a**; filled circles: Cu, empty circles: acetone. Top: view almost perpendicular to the cylinder axis; bottom: view onto the least-squares plane of the acetal oxygen atoms; the two acetone molecules depicted are the only guests inside the cylinder. Distances (pm) (cf. Scheme 4 for atom numbering): from Cu1 to: O307 189.6(6), O301 190.1(6), O207 194.1(6), O201 197.2(6); from Cu2 to: O310 191.0(5), O304 192.6(6), O204 194.0(5), O210 194.2(5); distances (pm) for **3b**: from Cu1 to: O307 187.4(8), O301 188.9(8), O207 193.9(8), O201 198.3(8); from Cu2 to: O310 190.2(7), O304 193.0(7), O204 193.2(7), O210 195.0(7).

established at the expense of type ***b*** bond lengths, resulting in the three-membered hydrogen-bond chains of Scheme 4 (note the large ***a***–***b*** difference of **3** compared with **1** and **2**, but bear in mind the overall mean of the O–H···O⁻ bond length, which is a true constant throughout the entire series of compounds in this work).

On the other hand, essentially the same geometric parameters are found for the dicuprate cylinders of both **3a** and **3b** despite the higher charge density of the potassium ions. Moreover, half of the rubidium ions of **3b** are disordered, thus further decreasing the charge density in the vicinity of the cuprate cylinders. All in all it is concluded that the influence of cuprate alkali contacts is diminished and the structure of the D_2 symmetrical anions is controlled – besides through Cu–O bonding – essentially by intramolecular hydrogen bonds. Accordingly, multidentate contacts of counterions and individual cuprate cylinders, typical for the structures of the tricuprates, are missing in **3**. The number of contacts of each of the potassium ions to an individual cuprate cylinder does not exceed three (legend of Figure 6). As in the case with **1** and largely with **2**, all of these contacts are of the type A···OH and no A···O⁻ bonds are present.

Metrical aspects: The characteristics of an α-cyclodextrin ligand may be represented by specifying significant geometrical quantities. In Table 3 a "cone base angle" and its standard deviation is

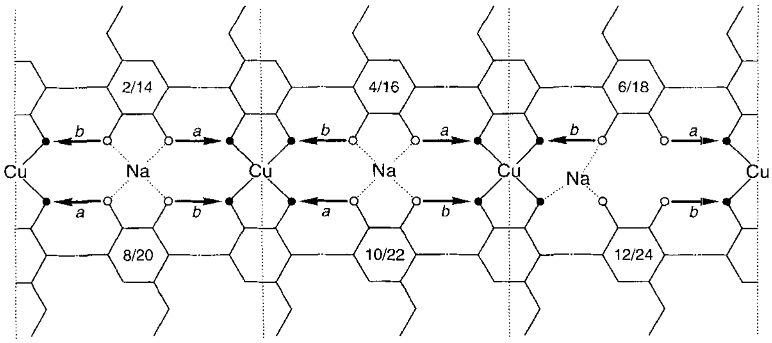

Scheme 3. Intramolecular hydrogen bonds and cyclodextrin numbering scheme in the structure of the cuprate(II) ions in **2**, depicted as arrows from donor to acceptor groups; donor-acceptor distances for ***a*** (O2 donors) and ***b*** (O3 donors) are given in Table 2.

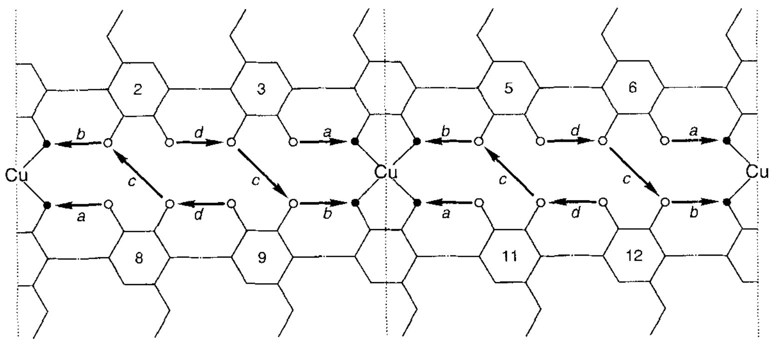

Scheme 4. Intramolecular hydrogen bonds and cyclodextrin numbering scheme in the structure of the cuprate(II) ions in **3**, depicted as arrows from donor to acceptor groups; donor-acceptor distances for ***a***–***d*** are given in Table 2.

Table 3. Mean values and standard deviations of the mean of geometrical parameters. Positional and cell parameters for α-cyclodextrin have been taken from K. K. Chacko and W. Saenger (cited in Figure 4).

	1	**2**	**3a**	**3b**	α-CD·7.57 H_2O
H-bonded O–O distance (pm)	266 ±6	268 ±11	281 ±19	281 ±19	298 ±8
cone base angle (°) [a]	88.0±1.3	84.4±4.6	87.2±1.6	87.6±1.7	78.7±9.3
acetal bond angle (°)	118.9±1.6	119.6±2.0	119.8±1.4	119.3±1.4	118.4±0.7
pyranose puckering amplitude (pm) [b]	57.1±1.9	55.8±2.3	56.0±1.6	56.1±1.9	56.1±1.0
bisdiol twist angle (°) [c]	17.4±6.0	21.0±4.5	11.4±5.9	11.7±5.8	
Cu-bonded diols only (°) [c]	11.8±1.7	21.6±3.9	3.2±1.6	3.7±2.1	
non-Cu-bonded diols only (°) [c]	23.0±2.5	20.4±5.0	15.4±1.0	15.7±1.0	

[a] Angle of least-squares planes defined by the pyranose ring atoms C1, C2, C3, C4, C5, O5 (plane 1) and by the acetal O atoms of the respective cyclodextrin ring (plane 2); defining plane 2 by copper atoms results in slightly different values: 88.2±1.3 (**1**), 85.8±4.1 (**2**). [b] D. Cremer, J. A. Pople, *J. Am. Chem. Soc.* **1975**, *97*, 1354–1358; only the puckering amplitudes are listed, since $\theta < 8°$ for most of the pyranose rings; larger θ values (°) have been calculated for anhydroglucose units with number: 2, $\theta = 9.5(17)$, $\phi = 42(10)$; 9, $\theta = 8.2(21)$, $\phi = 89(18)$; 11, $\theta = 8.7(17)$, $\phi = 95(10)$; 18, $\theta = 11.4(16)$, $\phi = 68(7)$ (**1**); 3, $\theta = 14(2)$, $\phi = 56(9)$; 5, $\theta = 9(2)$, $\phi = 83(12)$; 8, $\theta = 13(2)$, $\phi = 13(12)$; 16, $\theta = 11(2)$, $\phi = 90(14)$; 21, $\theta = 9(2)$, $\phi = 83(16)$ (**2**); 8, $\theta = 15.2(9)$, $\phi = 65(3)$; 11, $\theta = 12.7(9)$, $\theta = 76(4)$ (**3a**); 6, $\theta = 8.6(12)$, $\phi = 87(8)$; 8, $\theta = 12.8(13)$, $\phi = 75(5)$; 11, $\theta = 14.2(12)$, $\phi = 74(5)$ (**3b**). [c] The angle between the O–O vectors of two facing diol moieties in a double torus.

introduced as a measure of the shape and regularity of a cyclodextrin torus. The numerical values illustrate the formation of regular cyclodextrin cylinders (cone base angle ≈ 90°) on complexation, which may be compared with the more conical shape of free α-cyclodextrin in the 7.57 hydrate, which is the polymorph with the least collapsed cyclodextrin rings (Figure 5). Hence, complexation of the rather flexible[11] cyclodextrin rings obviously does not impose steric strain on the cyclic ligand. Neither the geometry of the anhydroglucose unit nor that of the acetal links indicates an unfavourable distortion (cf. Table 3, entries "acetal bond angle" and "pyranose puckering amplitude" which have been selected as being representative variables). This holds true even for the torsion angles ϕ (O4″···C1-O1-C4′) and ψ (C1-O1-C4′···O1″), which are close to 180°.

Figures 1–3 qualitatively show a distinct deviation of the environment of the copper atoms from a square planar one. This deviation may be expected, since the O2 atom of an O2/O3 ligator pair is more distant from the cylinder axis than O3 (Scheme 5). Thus, fitting two cyclodextrin tori facing their O2/O3 rims in a double-toroidal position suitable for coordination of metal ions, the two O2–O3 vectors will enclose a "bisdiol angle" (δ), which may be assessed from Scheme 5 to range between 12 and 14° (neglecting interdiol hydrogen bonding which, in the case of the α-cyclodextrin polymorphs, decreases O2 elevation; cf. Figure 4, bottom). As a result, square-planar coordination ($\delta = 0$) will be distorted towards a tetrahedral one ($\delta = 90°$), and a trigonal prism formed from both a bisdiol O_4 ligator set ($\delta = 0°$) and two further ligands will be distorted towards a *cis*-octahedron ($\delta = 60°$). Fivefold coordination is expected to be most variable, a square pyramid ($\delta = 0°$, the O_4 ligator set forming the basal square) being not too far away from a trigonal bipyramid ($\delta = 41.4°$) in terms of δ.

In fact, the structures of **1** and **3** exhibit the expected features. Thus, small bisdiol angles corresponding to square planar coordination are found at the copper site, while larger angles are observed with non-copper-binding diol couples. In particular the lithium ions in **1** adopt a favourable coordination midway between square pyramidal and trigonal bipyramidal coordination when including a water molecule as a further ligand. In **2**, all bisdiol angles are uniformly larger, ranging around 20° for both cupric and sodium binding sites. Examination of the individual angles reveals no significant difference between the angles next to the in-cylinder sodium atom and those in the vicinity of the out-of-cylinder ones. Thus, in terms of the bisdiol angle, **2** does not adopt a **1**-type structure with an irregularity at only one particular sodium site. Furthermore, each of the cyclodextrin-bound sodium ions try to attain a favourable octahedral coordination.

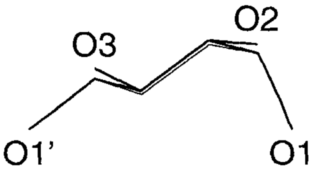

Scheme 5. The elevation of O2 with respect to the axis of a cyclodextrin torus (C6 and O6 omitted). The orientation resembles the one of the lower cyclodextrin rings in the bottom views of Figures 1–3.

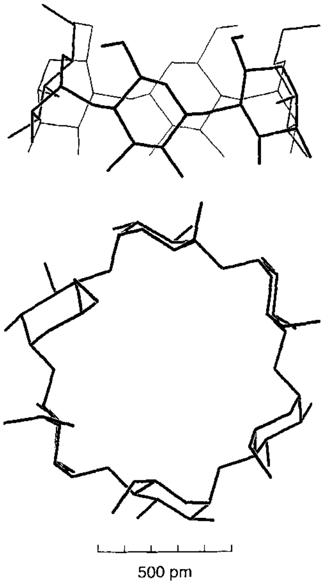

Figure 4. SCHAKAL drawing showing the conical shape of the α-cyclodextrin torus in the 7.57 hydrate polymorph (cf. the cyclodextrin cylinders in the cuprates); water molecules have been omitted; positional and cell parameters have been taken from K. K. Chacko and W. Saenger, *J. Am. Chem. Soc.* **1981**, *103*, 1708–1715.

Crystal structures: Having the highest water content of the four cuprates investigated, the tricuprate cylinders of **1** display the greatest separation in the solid state and thus exhibit an irregular arrangement in the crystal. If the individual tricuprate cylinders are considered to be large spheres, double hexagonal sphere packing (ABACAB...) can be recognized, with [010] as the stacking axis (compare the roughly hexagonal unit cell parameters in Table 1). The threefold pseudosymmetry of the cylinder arrangement cannot be traced back to the noncrystallographic symmetry of the individual cylinders, since the molecular $C3$ axes are heavily (≈ 55°) inclined away from the [010] axis.

The lower water content of **2** and **3** correlates with a more regular packing of the cylindrical anions in these compounds. The cuprate cylinders are stacked in a roll-of-coins-type mode in both structures, the individual stacks being arranged in a distorted hexagonal (**2**) or a tetragonal (**3**) rod packing, respectively (Figures 5 and 6). Stacking is staggered, such that the deprotonated central region of each of the cylinders is surrounded by the O6 ends of their neighbours. However, this stacking mode gives rise to O6–H···O$^-$ bonds on a large scale only for the water-poorer compound **3**, whereas in **2** the distinct separation of the stacks by both water and hydrated sodium ions allows only one contact of this kind.

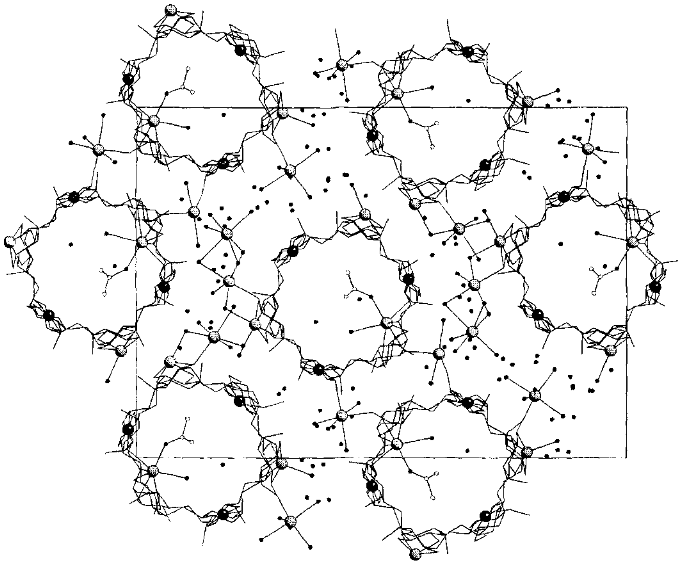

Figure 5. SCHAKAL drawing of **2**. Packing diagram, projection axis: [100]; filled circles: Cu; filled dots: water and acetone oxygen atoms; medium: Na, light: acetone carbon atoms; Na–O contacts <285 pm are drawn. Coordination of the sodium atoms [contacts >280 pm are given in square brackets]: two outside-bonded Na atoms in each of the two symmetrical independent cylinders (Na1, Na2, Na7, Na8): 4CD–OH2/3 +1-2H_2O; one inside-bonded Na atom in each cylinder (Na3, Na9): 1CD–O$^-$ +2CD–OH2/3 +1 acetone–O +1H_2O [+1 acetal–O +1CD–OH2]; Na4: 1CD–O6 +4H_2O +1CD–O$^-$; Na5: 5H_2O [+1CD OH2]; Na6 and Na10: 1CD–OH2 +5H_2O; Na11: 1CD–OH2 +1CD–O6 +5H_2O; Na12: 6H_2O; mean Na–O distance (distances <280 pm are based on averaging): 243.1 ± 12.9 pm.

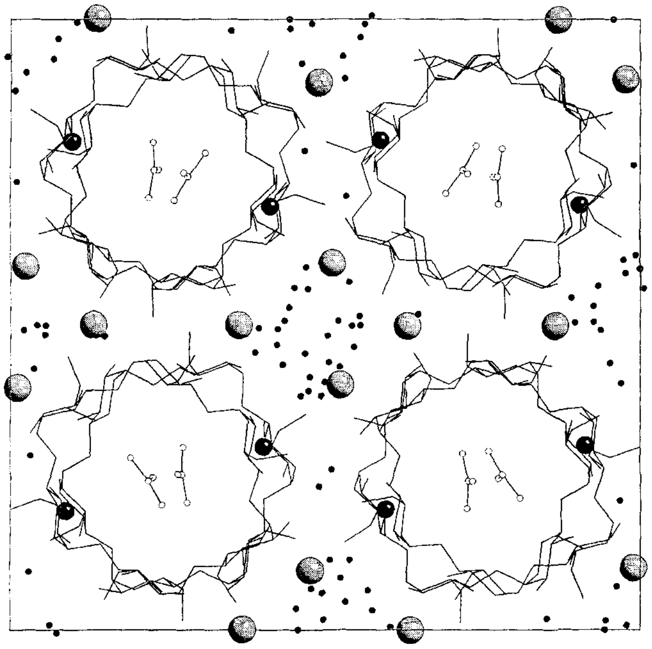

Figure 6. SCHAKAL drawing of **3a**. Packing diagram, projection axis: [0$\bar{1}$0]; filled circles: Cu; filled dots: water oxygen atoms; medium: K, light: acetone atoms; coordination of the potassium atoms: K1: 2CD–OH2/3 +2CD′–OH2/3 +3H_2O; K2: 3CD–OH2/3 +3CD′–OH2/3 +2H_2O; K3: 3CD–OH2/3 +1CD′–OH6 +4H_2O; K4: 1CD–OH2/3 +1CD′–O5 +1CD′–OH6 +4H_2O; mean K–O distance: 289.8 ± 15.2 pm.

Projections along the main axis of the cyclodextrin ligands illustrate the separation of hydrophilic and hydrophobic regions in the crystalline state. This principle is particularly obvious in **3**, in which both counterions and water molecules are found exclusively outside of the dicuprate cylinders, the interior of which (more precisely: both ends of each individual cylinder) serves as a host for acetone molecules (Figure 5). Thus, even the enhanced polarity due to the presence of two dianionic cuprate moieties in each of the cylinders of **3** obviously leaves the cyclodextrin cavity more hydrophobic than the outside, that is, the entire assembly of two copper-linked cyclodextrin tori resembles free α-cyclodextrin in this respect. On the whole, this statement also holds true for the tricuprate cylinders of **1** and **2**. For **2**, Figure 6 shows the huge number of water molecules in the interspace of the cyclodextrin rods, despite the unique sodium ion inside the cavity interfering with the prevailing hydophobic character of the cage.

The relatively high water content of **1**–**3** may be understood as a consequence of the presence of ionic groups. Most water molecules incorporated in the crystal structures of **1**–**3** serve as hydrogen-bond donors towards O$^-$ acceptors (generally, there are two hydrogen bonds formed by each of the alkoxide functions, one of those being an intramolecular bond and the second one being formed by tightly bound, well-ordered water molecules). As an example, this may be quantified for **2**. Here, almost all of the O$^-$ functionalities are not only acceptors in intramolecular hydrogen bonds but they also bind one additional water molecule each (mean H_2O···O$^-$ distance: 272 ± 11 pm). Subtracting both the alkoxide-bound and the sodium-coordinating water from the entire water content, only 6.5 H_2O (mostly O6-bonded) per α-cyclodextrin ring remains, which falls in the range of 6 to ca 7.5 H_2O for the α-cyclodextrin hydrate polymorphs.

Discussion

Deprotonated α-cyclodextrin as a ligand: On deprotonation and metal coordination, the hydrogen bond system of the cyclodextrin ring, which is responsible for the shape of the oligosaccharide cone, reorganizes itself. Thus, the formation of a polyolato complex imposes a characteristic change in shape on the cyclodextrin torus, which reflects the overall change of hydrogen bond length. In **1**–**3**, an overall shortening of the hydrogen-bonded O2···O3′ contacts pulls the formerly wide rim of the cyclodextrin cone to a smaller diameter, thus causing the cylindrical shape depicted in Figures 1–3, and can be quantified in terms of the cone base angle (Table 3).

The importance of steric factors should be emphasized: the metal-binding properties of a biscyclodextrin assembly may be most seriously affected by the actual bisdiol angle at a specific bisdiol pair. For **1**, the variability of the bisdiol angle permits suitable coordination of both cupric and lithium ions. However, the situation in **2** is less favourable for both cation types. A generally large bisdiol angle of ca. 20° at each metal binding site reflects the fact that neither is a favourable coordination of the cupric ions achieved nor are the trigonal prisms of the sodium ligators efficiently turned towards a *cis*-octahedral site. The question arises as to why an obviously more simple and symmetric structure that is easily derived from the lithium homologue is not realized, namely binding of three equivalent sodium ions in octahedral coordination formed from a $\delta \approx 0°$ $(OH)_4$ ligator set and two *trans* aqua ligands. However, the inconsistency of this apparently most suitable alternative becomes evident on inspection of the properties of the cyclodextrin cavity.

The hydrophobic character of the cavity of an uncomplexed cyclodextrin gives rise to the large number of known inclusion compounds with hydrophobic guests. Inspection of the very water-deficient cavities of **1** and **3** demonstrates that a marked hydrophobicity is obviously present even in the anionic cylinders. Thus, of the six aqua ligands of three *trans*-octahedra, those three ligands located inside the cavity would be in an unfavourable bonding state owing to the lack of further easily available water molecules with which they can form hydrogen bonds.

Cooperative counterion–guest assembling: In the actual structure of **2** this problem has been overcome by the intercalation of a more polar acetone guest, which not only fits well into the hydrophobic environment of the cavity but is also a suitable ligand for a sodium ion (due to the restricted space inside the cavity three acetone guests in common would be too bulky to intercalate, which explains the asymmetrical structure of **2**). On the other hand, the concomitant advance of an acetone molecule and two water molecules (Figure 2) into the belt region of the cuprate cylinder reflects the enhanced polarity of that region due to the shift of one of the sodium ions from the outer surface of the cylinder towards the cavity.

From a more speculative point of view, the different bonding modes of the acetone guests in **2** and **3** may be interpreted as being "snapshots" of a dynamic process, so that α-cyclodextrin provides, once again,[13] a vivid model for an elementary reaction step inside the hydrophobic cavity of an enzyme. The bonding situation of acetone in **3** may be considered as a starting point; van-der-Waals-bonded acetone guests are loosely fixed at the entrance of a hydrophobic cage. In **2**, both a slight dislocation of a sodium atom towards the cavity and movement of an acetone molecule deeper into the host transform the van-der-Waals-type host–guest interaction of **3** into a well-defined coordinative bond. The new $Na^+ \cdots O$ contacts are forming in a region of variable polarity, which itself depends on the actual spatial arrangement of the mobile polar entities.

Conclusions

With respect to polyolatocuprate formation, the most striking difference between simple polyols and cyclodextrins is the larger number of cupric ions bound by a given quantity of diol groups in the former. Instead, cyclodextrin diol moieties contribute to intramolecular hydrogen bonds at the expense of polyolatometallate formation. Proceeding from the extensive hydrogen-bond structure of an uncomplexed cyclodextrin, progressive deprotonation on complexation together with concomitant remodelling of the shape of the cyclodextrin torus may be seen in the light of reorganization processes of an increasingly proton-deficient hydrogen-bond system. Reconsidering the issues of this investigation, one may derive some preliminary rules of oligosaccharide–metal complexation:

1) Full deprotonation and metal ligation of diol functions may be limited if there is competitive intramolecular hydrogen bonding (note the peculiar quality of the polysaccharide cellulose in forming hydrogen bond-supported diolate ligators without having to use the diol functions as donor groups[1]).
2) Direct $A^+ \cdots O^-$ contacts, common in simple polyolatocuprates, are largely absent. Instead, polarized intramolecular chains $A^+ \cdots (O{-}H)_n \cdots O^-$ are formed; $n > 1$ is observed for weakly polarizing, large cations, $n = 1$ is common for Li^+ and Na^+. Particularly tight counterion binding may arise if multidentate cation binding sites are assembled, for example hydroxylic O_4 ligator sets for Li^+, which may easily be capped to fivefold coordination. The contribution of the counterions to the structure of the oligosaccharide copper complex is tightly restricted to the smaller, efficiently polarizing cations.
3) On the other hand, counterions with the charge density of the heavier alkali cations that are incorporated into $A^+ \cdots (O{-}H)_n \cdots O^-$ chains appear to be roughly equivalent to a further water donor like $HO{-}H \cdots (O{-}H)_n \cdots O^-$ in an aqueous environment.

On the whole, it may be stated that the formation of a specific oligosaccharide–metal assembly strongly depends on both the counterion and the polyolate-ligating metal. To focus on the significance of the guest molecules inside the cavity, and in the light of a recent classification of the main types of interactions in supramolecular building units,[14] a metal–cyclodextrin assembly demonstrates all of the basic bonding modes (nonspecific van-der-Waals bonds, hydrogen bonds, ligand-to-metal bonds) in a single molecular system.

Acknowledgements: This work was supported by the Bundesministerium für Ernährung, Landwirtschaft und Forsten (Fachagentur Nachwachsende Rohstoffe), grant 95NR111-F; α-cyclodextrin was donated by Wacker-Chemie, München.

Received: October 7, 1996 [F483]

---

[1] W. Burchard, N. Habermann, P. Klüfers, B. Seger, U. Wilhelm, *Angew. Chem.* **1994**, *106*, 936–939; *Angew. Chem. Int. Ed. Engl.* **1994**, *33*, 884–887.

[2] N. Habermann, M. Klaassen, P. Klüfers, *Carbohydr. Res.* **1993**, *241*, 9–23; N. Habermann, G. Jung, M. Klaassen, P. Klüfers, Chem. Ber. **1992**, *125*, 809–814; M. Klaassen, P. Klüfers, *Z. Anorg. Allg. Chem.* **1993**, *619*, 661–666; M. Klaassen, P. Klüfers, *Acta Crystallogr. Sect. C* **1994**, *50*, 686–688; M. Klaassen, P. Klüfers, *Z. Anorg. Allg. Chem.* **1994**, *620*, 1631–1634.

[3] C. Gack, P. Klüfers, *Acta Crystallogr. Sect. C* **1996**, *52*, 2972–2975.

[4] P. Klüfers, H. Piotrowski, J. Schuhmacher, *Z. Anorg. Allg. Chem.* **1997**, *623*, 191–199.

[5] Compare with the structures of the cuprates formed with the isomeric hexitols dulcitol (P. Klüfers, J. Schuhmacher, *Angew. Chem.* **1994**, *106*, 1839–1841; *Angew. Chem. Int. Ed. Engl.* **1994**, *33*, 1742–1744) and D-sorbitol (P. Klüfers, J. Schuhmacher, *Angew. Chem.* **1995**, *107*, 2290–2292; *Angew. Chem. Int. Ed. Engl.* **1995**, *34*, 2119–2121).

[6] G. v. Sengbusch, H. D. Lemke, J. Viencken, in *Uremia Therapy* (Ed.: H. J. Gurland), Springer, Berlin, **1987**, pp. 111–124.

[7] F. Hoelkeskamp, *Papier (Darmstadt)* **1962**, *16*, 102–105; *ibid.* **1964**, *18*, 201–204.

[8] For an account of the difficulties in obtaining crystalline cellodextrins (K. Gessler, N. Kraus, T. Steimer, C. Betzel, C. Sandmann, W. Saenger, *Science* **1994**, *266*, 1027–1029).

[9] a) R. Fuchs, N. Habermann, P. Klüfers, *Angew. Chem.* **1993**, 105, 895–897; *Angew. Chem. Int. Ed. Engl.* **1993**, *32*, 852–854; b) for the structure of a lead(II) complex of γ-cyclodextrin see: P. Klüfers, J. Schuhmacher, *ibid.* **1994**, *106*, 1925–1927; **1994**, *33*, 1863–1865.

[10] Further details of the crystal structure investigation may be obtained from the Fachinformationszentrum Karlsruhe, D-76344 Eggenstein-Leopoldshafen (Germany), on quoting the depository numbers CSD-405771 (**1**), CSD-405770 (**2**), CSD-405769 (**3a**) and CSD-405768 (**3b**).

[11] K. B. Lipkowitz, *J. Org. Chem.* **1991**, *56*, 6357–6367.

[12] Compare this with the clockwise rotation of uncomplexed anhydroglucose rings (the sense of rotation refers to a lateral view from the cylinder side towards the cavity) in two hydrates of $Li_{11}[Cu_4(\beta\text{-CDH}_{-9.5})_2]$ establishing O2···O2 hydrogen bonds: R. Fuchs, N. Habermann, P. Klüfers, *Angew. Chem.* **1993**, *105*, 895–897; *Angew. Chem. Int. Ed. Engl.* **1993**, *32*, 852–854.

[13] G. A. Jeffrey, W. Saenger, *Hydrogen Bonding in Biological Structures*, Springer, Berlin, **1991**, p. 312; the authors interpret structural changes of cyclodextrin hosts on forming inclusion compounds in terms of an induced-fit mechanism exhibited by enzymes.

[14] D. Philp, J. F. Stoddart, *Angew. Chem.* **1996**, *108*, 1243–1286; *Angew. Chem. Int. Ed. Engl.* **1996**, *35*, 1154–1196.